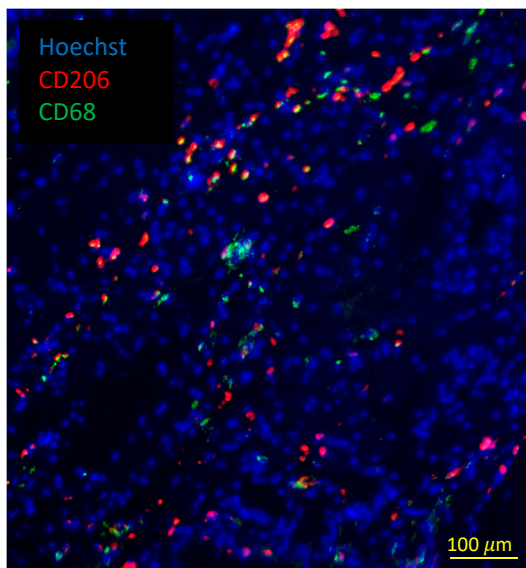


Supplementary data

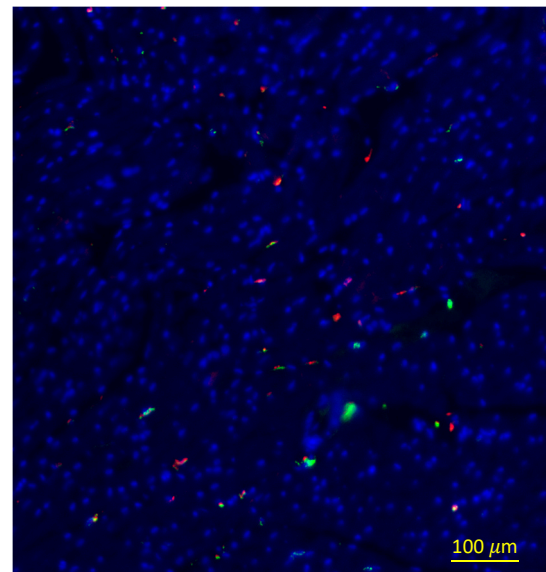
Fibrin, Bone Marrow Cells and macrophages interactively modulate cardiomyoblast fate.

Inês Borrego ¹, Aurélien Frobert ¹, Guillaume Ajalbert ¹, Jérémy Valentin ¹, Cyrielle Kaltenrieder¹, Benoît Fellay ³, Michael Stumpe², Stéphane Cook ^{1,3}, Joern Dengjel ², Marie-Noelle Giraud ¹ *

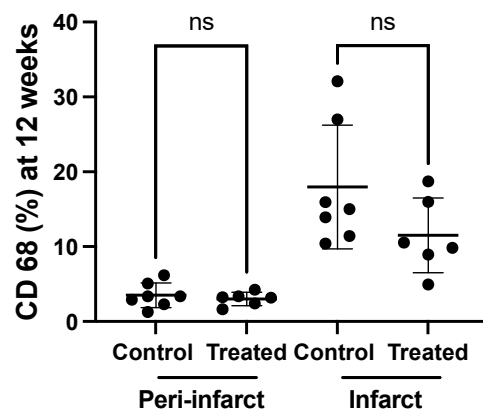
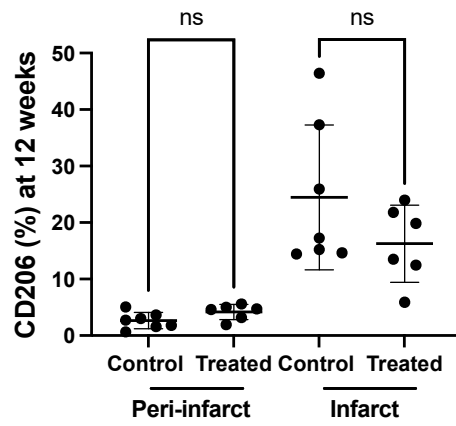
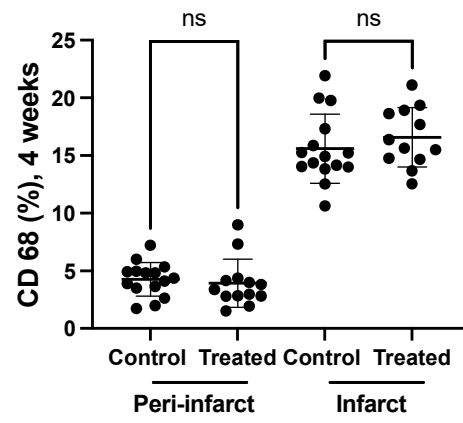
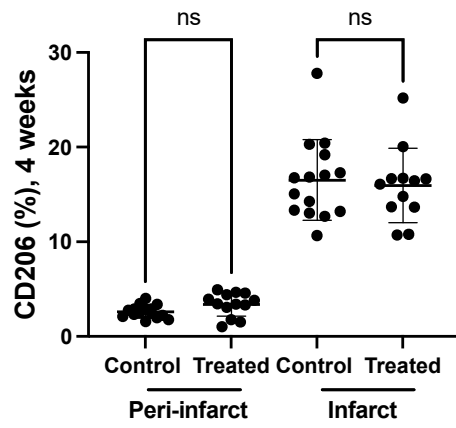
Figure S1: CD68+, CD206+ macrophages within the infarcted area and border zone were similar in all groups. Immunostainings for CD206 (A, C) and CD68 (B, D) were performed on paraffin-embedded heart sections. 5 to 6 cross-sections from a systematic sampling of the whole heart were averaged for each animal. Hearts were harvested 4 or 12 weeks post-treatment.



Infarct area



Peri-infarct area

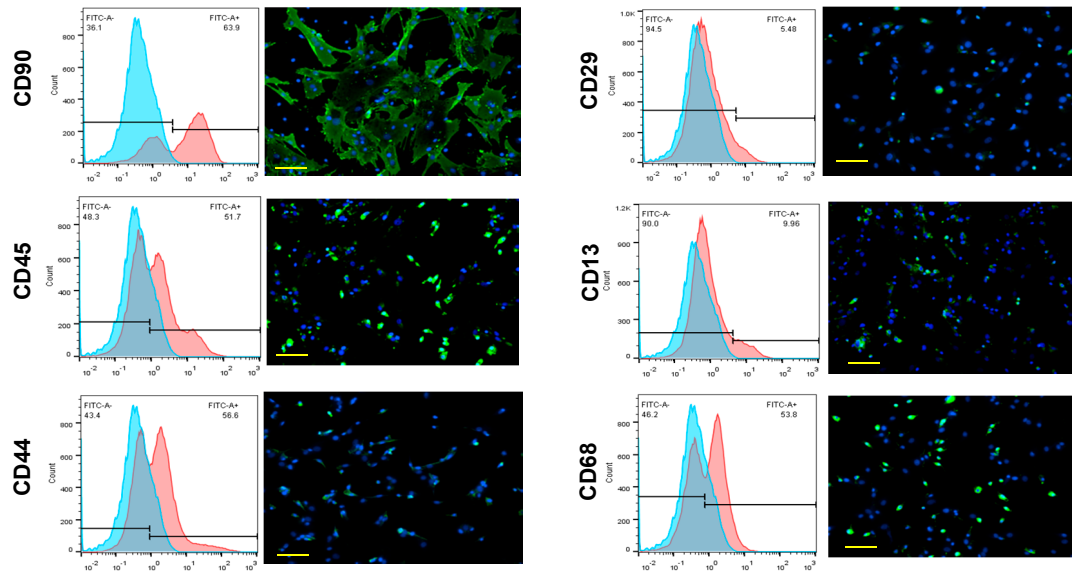


Methods:

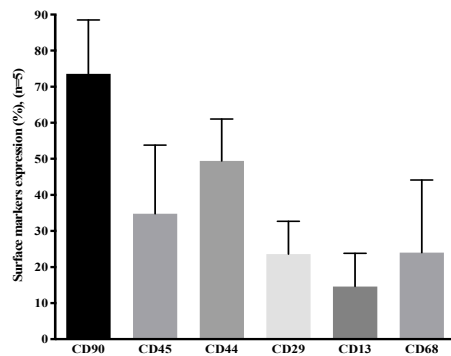
Macrophages immunohistochemistry: Samples from rat hearts sectioned into 5-6 parts starting at the base and going to the apex were used for double fluorescent immunochemistry staining. Anti-CD206 (Abcam, ab64693) and anti-CD68 (Abcam, ab31630) were used as primary antibodies and Donkey anti-Rabbit Alexa Fluor® 647 (Abcam, ab150075) and Goat anti-mouse Alexa Fluor® 488 (Abcam, ab150113) were used as secondary antibodies. The tissue sections were counterstained with Hoechst. Images of the left ventricle were acquired using a DM6B bright-field microscope (Leica) at 10x magnification. The quantification was done on FIJJ (ImageJ). Two regions within the infarct zone and the adjacent infarct zone were delimited for each image. An auto-threshold was performed. On each region of interest (ROI), the number of CD206 and CD68 positive cells, Hoechst stained nuclei and the total area covered by these cells were automatically counted. Each image's masks were inspected manually to verify the automatic counting. CD206⁺ and CD68⁺ cells ratio was calculated by dividing the number of CD206⁺ or CD68⁺ cells by the total nuclei for each ROI.

Figure S2: Surface markers of BMCs measured by flow cytometry and immunostaining. (A) Histogram represents the flow cytometry results, and the pictures represent the immunostainings of the cells. Scale bar represent 100 μ m. BMC are a heterogeneous population of cells as indicated by markers from the mesenchymal (CD90, CD29, CD13) and hematopoietic (CD45, CD44, CD68) lineages. The mesenchymal CD90⁺ cells were most abundant. They form a population of large and spread cells. (B) Quantification of the immunostainings

A



B



Methods:

Five different pools of BMC (pools of 10 or 3 animals) used in this study were characterised by flow cytometry. Passage 2 cells were detached with accutase. Cell surface markers were analysed using unlabelled Anti-CD90 (rabbit; ab225; Abcam, United Kingdom), anti-CD45 (ab10558, RRID:AB_442810, Abcam, United Kingdom), anti-CD44 (ab119348, RRID:AB_10902529, Abcam, United Kingdom), anti-CD29 (ab179471; RRID:AB_2773020, Abcam, United Kingdom), anti-CD13 (ab108310, RRID:AB_10866195, Abcam, United Kingdom) and anti-CD68 (ab31630, RRID:AB_1141557, Abcam, United Kingdom) in 1:50 dilution. Cells were

further labelled with a secondary antibody (1:500 dilution), including Alexa Fluor 488-conjugated anti-rabbit (ab150077, RRID: AB_2630356, Abcam, United Kingdom), Chromeo 488-conjugated anti-mouse (ab60313, RRID: AB_954967, Abcam, United Kingdom) and FITC-conjugated anti-rat (ab6730, RRID: AB_955327, Abcam, United Kingdom). Stained cells were fixed with 1% Para-Formaldehyde and stored at 4 °C until further analysis. Negative controls without primary antibodies were included. Flow cytometry was performed, and cell surface markers expression was acquired on a MACSQuant® Analyser 10 (Miltenyl Biotec, Germany) instrument, and the data were analysed using the FlowJo 10.4.2 (Flowjo Cloud, USA) software.

Furthermore, BMC cultured in tissue culture chamber (Sarsted, Mümbrecht, Germany) and fixed with paraformaldehyde 4% were characterised by immunostaining for CD90, CD45, CD44, CD29, CD13, CD68 according to the procedure described for flow cytometry. Cells were counterstained with Hoechst (1:200 dilution; Sigma-Aldrich, Switzerland) and examined under a high-resolution bright-field light microscope Nikon Eclipse Ni (Nikon, Japan), captured using a Nikon Digital Sight DS – Ri 1 camera and analysed by Nikon NIS elements software (Nikon, Japan).

Figure S3: Comparison of the expression profiles of macrophages cultured in F-BMC, BMC or fibrin conditioned medium.

Fold changes (FC) in gene expressions of pro- and anti-inflammatory markers were calculated for educated macrophages ($M_{(-)}$, $M_{(LPS, IFN)}$ or $M_{(IL4)}$) relative to uneducated ones. The values shown are mean \pm SD. All $n=3$ biologically independent samples constituted of macrophages pools, each pool was obtained from 3 animals, therefore, 9 animals per group. Statistics were performed using two-way ANOVA and a turkey's multiple comparison test as a post hoc test to compare a single effect for each macrophage subset and each gene.

For $M_{(IL4)}$, the downregulation of pro-inflammatory and upregulation of anti-inflammatory genes were similar when educated with F-BMC, BMC or fibrin except for *Cd163*, *Nos2* and *Mcp1*.

For $M_{(-)}$ and $M_{(LPS, IFN)}$, F-BMC induced significantly pronounced changes of *Arg1*, *Il10*, *Cd80*, *Tnfa* compared to fibrin. When compared to BMC, the significative changes are macrophage subset dependent. Significant differences were measured in $M_{(-)}$ for *TGFb*, *Il10*, *IL6* and *TNfa*. For $M_{(LPS, IFN)}$, the most pronounced effects were observed for *Arg1* and *Tnfa*. Notably, fibrin induced downregulation of pro- and anti-inflammatory genes principally.

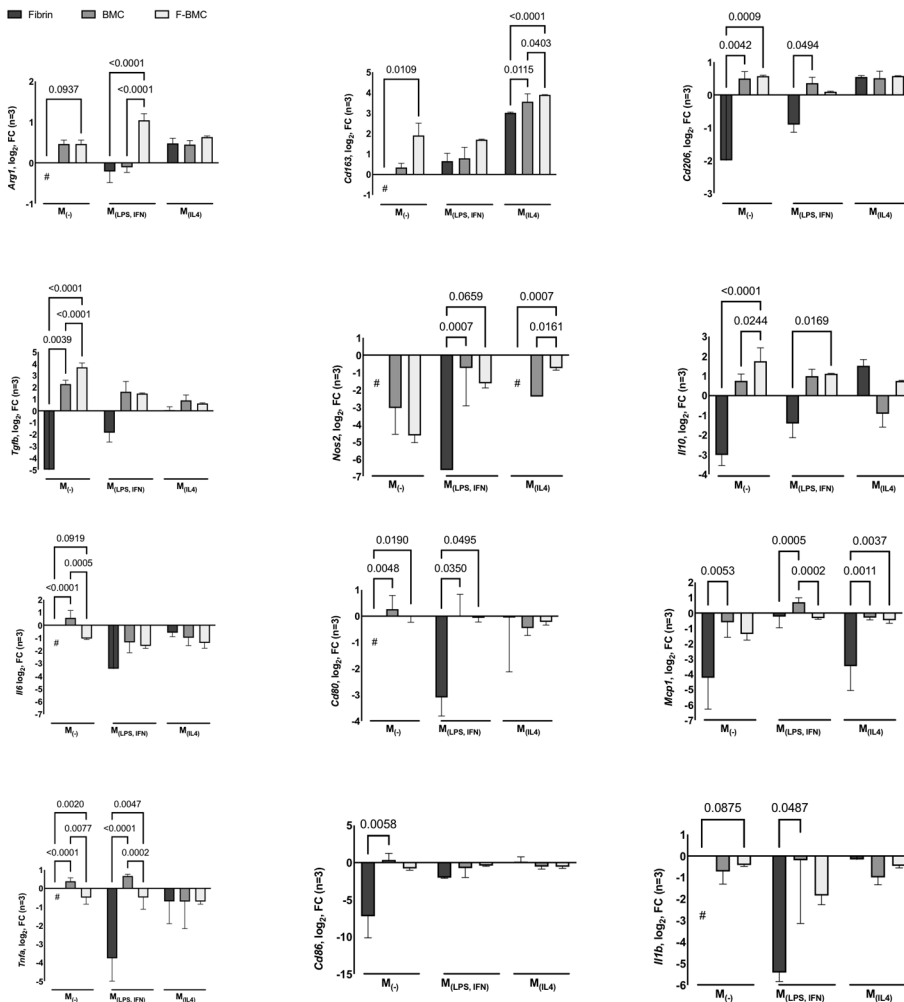


Table S2: Primers used for real-time PCR analysis

Gene	Forward Primer (5'-3')	Reverse Primer (5'-3')
<i>Arg 1</i>	TTGATGTTGATGGACTGGAC	TCTCTGGCTTATGATTACCTTC
<i>Arg2</i>	CGT CTC CCG TCT CCT CCA C	ACC ACC TCA GCC AGT TCC TG
<i>b-Actin</i>	AGCGTGGCTACAGCTTCACC	AAGTCTAGGGCAACATAGCACAGC
<i>Cd163</i>	TCAGCGTCTCTGCTGTCACCTCA	CGTTCATGCTCCAGCCGTTA
<i>Cd206</i>	TGTGAGCAACCACTGGGTTA	GTGCATGTTTGGTTTGCATC
<i>Cd80</i>	TCGTACGTGGTGAAACACCTGA	CCGGAAGCAAAGCAGGTAATC
<i>Cd86</i>	GACACCCACGGGATCAATTA	AGGTTTCGGGTATCCTTGCT
<i>Cxcl10</i>	TTC CGT AAG CTA TGT GCA GGT A	TCA GGT GAA CTC AGA ACT GAT G
<i>Gapdh</i>	TGCCCCCATGTTTGTGATG	GCTGACAATCTTGAGGGAGTTGT
<i>Gm-csf</i>	GCA GAC CCG CCT GAA GCT AT	CGG CTT CCA GCA GTC AAA AGG
<i>Icam1</i>	TGA GCG ACA TTG GGG AAG AC	TCG CTC TGG GAA CGA ATA CAC
<i>IFN gamma</i>	TCG CAC CTG ATC ACT AAC TTC TTC	CGA CTC CTT TTC CGC TTC C
<i>Il-1 beta</i>	GCACCTTCTTTTCCTTCATCTTTG	TTTGTCGTTGCTTGCTCTCTCCTT
<i>Il-10</i>	CTGTCATCGATTTCTCCCCTGT	CAGTAGATGCCGGGTGGTTC
<i>IL-1a</i>	AAG ACA AGC CTG TGT TGC TGA AGG	TCC CAG AAG AAA ATG AGG TCG GTC
<i>IL-1ra</i>	TCTGCAGGGGACCTTACAGT	GGTCTTCTGGAAGTAGAAC
<i>Il-4</i>	ACC TTG CTG TCA CCC TGT TCT	AGC TCG TTC TCC GTG GTG T
<i>Il-6</i>	AAATGGTCCCCGGAGGT	AAGACACAGAGAGAAGCAATCCAAAC
<i>iNos</i>	ATGGAACAGTATAAGGCAAAC	GTTTCTGGTCGATGTCATGAG
<i>M-csf</i>	GGG AAT GGA CAC CTA CAG ATT TTG	AAA TTT ATA TTC GAT CAG GCA TGC A
<i>Mcp-1</i>	CTA TGC AGG TCT GTC ACG CTT C	CAG CCG ACT CAT TGG GAT CA
<i>Mmp3</i>	TCT TTC ACT CAG CCA ATG CT	GGG AGG TCC ATA GAG GGA TT
<i>Mmp9</i>	AGC CGG GAA CGT ATC TGG A	TGG AAA CTC ACA CGC CAG AAG
<i>Rantes</i>	CGTGAAGGAGTATTTTACACCAGC	CTTGAACCCACTTCTTCTCTGGG
<i>TGF beta</i>	CTTCAGCTCCACAGAGAACTGC	CACGATCATGTTGGACAACTGCTCC
<i>Timpl</i>	CAG CAA AAG GCC TTC GTA A	TGG CTG AAC AGG GAA ACA CT
<i>TNF alfa</i>	TGCCTCAGCCTCTTCTCATTC	GCTCCTCTGCTTGGTGGTTT
<i>Vcam1</i>	ACA AAA CGC TCG CTC AGA TT	GTC CAT GGT CAG AAC GGA CT